Published in final edited form as:
*Free Radic Biol Med*. 2011 January 15; 50(2): 281–294. doi:10.1016/j.freeradbiomed.2010.11.006.

# Non-esterified Cholesterol Content of Lysosomes Modulates Susceptibility to Oxidant-induced Permeabilization

**John J. Reiners Jr**[a,*], **Miriam Kleinman**[a], **David Kessel**[b], **Patricia A. Mathieu**[a], and **Joseph A. Caruso**[a]

[a]Institute of Environmental Health Sciences, Wayne State University, Detroit, MI 48201

[b]Department of Pharmacology, Wayne State University School of Medicine, Detroit, MI 48201

## Abstract

Reactive oxygen species (ROS) can induce lysosomal membrane permeabilization (LMP). Photoirradiation of murine hepatoma 1c1c7 cultures preloaded with the photosensitizer NPe6 generates singlet oxygen within acidic organelles, and causes LMP and the activation of procaspases. Treatment with the cationic amphiphilic drugs (CADs) U18666A, imipramine, and clozapine stimulated the accumulation of filipin-stainable non-esterified cholesterol/sterols in late endosomes/lysosomes, but not in mitochondria. Concentration-response studies demonstrated an inverse relationship between lysosomal non-esterified cholesterol/sterol contents and susceptibility to NPe6 photoirradiation-induced intracellular membrane oxidation, LMP, and activation of procaspases-9 and -3. Similarly, the kinetics of restoration of NPe6 photoirradiation-induced LMP paralleled the losses of lysosomal cholesterol that occurred upon replating U18666A-treated cultures in CAD-free medium. Consistent with the oxidation of lysosomal cholesterol, filipin staining in U18666A-treated cultures progressively decreased with increasing photoirradiating light dose. U18666A also suppressed the inductions of LMP and procaspase activation by exogenously added hydrogen peroxide. However, neither U18666A nor imipramine suppressed the induction of apoptosis by agents that did not directly induce LMP. These studies indicate that lysosomal non-esterified cholesterol/sterol content modulates susceptibility to ROS-induced LMP, and possibly does so by being an alternative target for oxidants and lowering the probability of damage to other lysosomal membrane lipids and/or proteins.

### Keywords

PDT; photodynamic treatment; NPe6; lysosomal membrane permeabilization; LMP; lysosomes; cholesterol; apoptosis; reactive oxygen species; C11-BODIPY

## Introduction

Lysosomes play a critical role in protein, lipid and carbohydrate catabolism, plasma membrane recycling, lipid and sterol trafficking, antigen processing, and autophagy. These processes are mediated by a variety of organelle-contained hydrolytic activities. Disruption



*Corresponding author: John J. Reiners, Jr., Institute of Environmental Health Sciences, Wayne State University, 259 Mack Ave., Rm 4114, Detroit, MI 48201, Telephone # (313) 577-5594, FAX # (313) 577-0082, john.reiners.jr@wayne.edu.

of lysosomal membrane integrity, and the release of lysosomal enzymes into the cytosol, can have grave cytotoxic consequences resulting in apoptotic or necrotic death [1–3]. Surprisingly, an extensive list of agents and physiological conditions are capable of inducing lysosomal membrane permeabilization (LMP). Among such agents and conditions are $H_2O_2$ [4,5], methylmercury [4], recycling quinines [6], photosensitizers that accumulate in lysosomes [7,8], UV irradiation [9], camptothecin, [10], cisplatin [11], etoposide [11–13], tumor necrosis factor alpha [11,14], TRAIL [15,16], hypoxia [16] and proteasome inhibitors [17].

The mechanisms by which the aforementioned agents induce LMP are largely unknown. Current hypotheses range from non-specific permeabilization caused by enzymatic- and/or oxidant-induced damage to lysosomal membrane lipids and proteins, to toxicant-induced formation of lysosomal pores or channels [1–3]. In the case of the former, several studies have implicated calpain, phospholipase $A_2$, and caspases as contributors to LMP [1]. As for the latter, LMP induction by TRAIL [15] or staurosporine [18] is paralleled by the association of activated Bax with the lysosomes in some model systems. This association appears to be essential because knockdown of Bax expression suppresses LMP [15,18]. Furthermore, TRAIL-induced LMP is suppressed by over expression of Bcl-2 or Bcl-xL [15]. Given the ability of Bax to permeabilize mitochondria via its formation of pores, it seems conceivable that a comparable effect may occur following its association with lysosomes.

A significant number of proteins have been implicated as regulators of LMP. Among such proteins are several anti-apoptotic members of the Bcl-2 family [1,15], phospho-p53$^{ser15}$ [19,20], LAPF [20], LAMP1 and 2 [13], HSP70 [9,12] and the aryl hydrocarbon receptor (AhR) [14,21]. In the case of the AhR, comparisons of wild type versus AhR-deficient variants indicated that the variants were resistant to induction of LMP by either TNFα [14] or photodynamic treatment (PDT)-induced intra organelle generated singlet oxygen [21]. Although the basis for the resistance of the variants was not determined, digitonin permeabilization studies led the authors to speculate that AhR-content may influence lysosomal cholesterol content [14]. Indeed, the sensitivity of isolated lysosome preparations to osmotic stress-induced rupture can be enhanced [22,23] or suppressed [23] by treatments that reduce or increase lysosomal membrane cholesterol content, respectively.

In the current study we assess whether lysosomal non-esterified cholesterol content modulates sensitivity to oxidant-induced LMP. We took advantage of previous findings that the photosensitizer NPe6 preferentially localizes to lysosomes, and that a very strong pulse of highly reactive singlet oxygen is generated within the organelle following exposure to red light [7]. Previous studies from our laboratory have shown that PDT protocols employing NPe6 rapidly induce LMP, cathepsin-mediated cleavage of Bid, release of cytochrome c, and activation of the apoptosome [7,21]. We also examined the effects of exogenously added $H_2O_2$, an oxidant that has multiple modes of pro-oxidant action, including the induction of LMP [4,5]. Modulation of lysosomal cholesterol content was achieved by treating cultures with varying concentrations of the cationic amphiphilic drugs (CADs) imipramine, clozapine, and U18666A. The ability of the latter drug to induce accumulation of lysosomal non-esterified cholesterol/sterols is well documented [24–27]. The current study demonstrates that lysosomal cholesterol/sterol content modulates susceptibility to oxidant-induced LMP. This property is of considerable significance given the numerous pharmaceutical, pathological and physiological conditions that facilitate lysosomal non-esterified cholesterol/sterol accumulation.

## Materials and methods

### Reagents

Ac-DEVD-AMC and AMC were obtained from BD Biosciences (San Diego, CA). HA14-1 was from Ryan Scientific (Isle of Palms, SC). Staurosporine, thapsigargin, $H_2O_2$, U18666A, imipramine and clozapine were obtained from Sigma-Aldrich (St. Louis, MO). NPe6 was a gift from Light Sciences (Issaquah, WA). Acridine orange, C11-BODIPY$^{581/591}$, LysoSensor Green DND-189, MitoTracker Green FM (fixable) and dextran 10,000 tetramethylrhodamine (lysine fixable) were purchased from Molecular Probes (Eugene, OR).

### Cell culture

Murine hepatoma Hepa 1c1c7 cells were obtained from Dr. J.P. Whitlock, Jr. (Stanford University, Stanford, CA) and grown in αMEM supplemented with 5% (v/v) fetal bovine serum and antibiotics in a 5% $CO_2$ atmosphere, at 37°C. Cultures were established in either commercial culture dishes or on poly-L-lysine-coated coverslips. Cells were plated at a density that ensured exponential growth for at least 4 days.

Cultures were generally treated 1–2 days after plating. Stock solutions and subsequent dilutions of clozapine, staurosporine, and thapsigargin were made in DMSO. Total solvent content never exceeded 0.1% (v/v). U18666A and imipramine were made in, and diluted with water. Stock solutions of $H_2O_2$ were diluted in ‘conditioned’ complete medium to achieve a desired final concentration immediately before transfer to test cultures. Conditioned medium was derived from 1c1c7 cultures that had been plated at the same time, and at the same density, as the cultures used for peroxide treatment. Culture medium was removed from conditioning plates and centrifuged. The resulting supernatant fluid was used as ‘conditioned’ medium. Use of ‘conditioned’ medium yielded very reproducible, quantitatively similar $H_2O_2$ inductions of LMP and DEVDase activation from experiment to experiment.

### Photodynamic therapy

NPe6 was dissolved in water the evening before PDT. For most of the reported studies cultures were loaded with 33 μM NPe6 for 1–2 h prior to washing, refeeding, and photoirradiation (1 s of irradiation corresponds to 1.5 mJ/cm$^2$). Photoirradiation was achieved with a 600 W quartz-halogen lamp with IR radiation attenuated with a 10 cm layer of water and an 850 nm cutoff filter. The exciting light was further restricted using a 660 nm long pass filter.

### DEVDase assay

Activation of procaspases-3 and -7 was analyzed by monitoring the generation of AMC from the caspase substrate Ac-DEVD-AMC. The procedures used for the harvesting of cells and measuring DEVDase activity have been described in detail [21]. Changes in fluorescence over time were converted into pmoles of product by comparison to a standard curve generated with AMC. DEVDase-specific activities are reported as nmol of product generated per min per mg of protein. The bicinchoninic acid assay, using BSA as a standard, was used to estimate protein concentrations.

### Western-blot analyses

The reagents and procedures used for the preparation and processing of cell lysates, SDS gel electrophoresis, and immunodetection of caspases-9 and -3 (pro- and active forms) and actin have been described in detail [7,21].

### Fluorescence microscopy

Most immunofluorescence studies employed cells growing on glass coverslips that had been precoated with poly-L-lysine. Unless noted otherwise, digital images were captured with either a Zeiss Axiovert 200M fluorescence microscope, or a Zeiss Axioplan 2 Imaging fluorescence microscope equipped with an ApoTome optical sectioning device. The latter microscope was used for the capturing of 0.5 or 1 μm Z plane images. All images were digitally captured and imported into Photoshop for cropping and sizing. Images within a figure subpanel were always taken using identical conditions (unless stated otherwise). Any post capture manipulations of images (brightness or contrast) were uniformly applied to all images within a panel group.

### Acridine orange staining of acidic organelles

Fifty min after irradiation cultures were incubated simultaneously with 500 nM AO ± 500 nM HO33342 for 10 min prior to being imaged sequentially using filter cubes that captured green (AO in neutral pH environment), red (AO in acidic pH environment), and blue (HO33342) fluorescence. Green fluorescence was detected using a filter set consisting of 490–510 nm excitation, 515 nm dichroic mirror, and 520–550 nm emission. Red fluorescence was detected employing 534–558 nm excitation, a 580 nm dichroic mirror, and a 590 nm long pass emission filter. Blue fluorescence was detected employing 365 nm excitation, a 395 nm dichroic mirror, and a 420 nm long pass emission filter.

### Colocalization of LAMP1 and cathepsin D

The reagents, antibodies, and procedure for immunofluorescence detection and colocalization of LAMP1 and cathepsin D in Z plane sections of 1c1c7 cultures have been described in great detail [14]. In brief, cathepsin D and LAMP1 were detected with a 1:20 dilution of rabbit anti-human cathepsin D antibody (Oncogene Research Products, San Diego, CA) and 1:1000 dilution of 1D4B rat anti-mouse LAMP1 antibody (Development Studies Hybridoma Bank, Department of Biological Sciences, University of Iowa, Iowa City, IA), respectively. Secondary detection consisted of incubation with 1:200 dilutions of AlexaFluor 488 goat-anti-rabbit IgG and AlexaFluor 546 goat anti-rat IgG (Molecular Probes).

### Filipin staining of non-esterified sterols

In order to detect non-esterified cholesterol/sterols, cultures were washed 3x with PBS and fixed with 4% paraformaldehyde/PBS (w/w) for 30 min at room temperature. After 3 washings with PBS the cells were incubated with 100 mM glycine/PBS for 10 min, and stained with filipin (9.05 mg/ml in 5% BSA/PBS (w/w)) for 2 h. All steps were performed at room temperature. Cells were subsequently washed with PBS and coverslips were inverted onto a drop of SlowFade solution on a glass slide. Digital images were captured with a Zeiss Axiovert 200M fluorescent microscope using a filter set consisting of 365 nm excitation, 395 nm dichroic mirror, and 420 nm long pass emission filter. Filipin was initially prepared in DMSO.

### Colocalization of Filipin and endosomes/lysosomes

Two protocols were employed to determine if filipin stained late endosomes/lysosomes. In the ‘direct’ procedure coverslips were washed with PBS and fixed as described above. After washing the coverslips three times with PBS the cells were incubated in a 4% BSA/PBS (w/w) solution for 1 h at room temperature to block non-specific immunoglobulin binding. Cells were then incubated with a 5% BSA/PBS (w/w) solution containing 1:1000 1D4B rat anti-mouse LAMP1 antibody and 9.05 mg/ml filipin, in the dark for 2 h at room temperature. The coverslips were subsequently washed with PBS followed by incubation

with a 1:200 dilution of AlexaFluor 546 goat anti-rabbit IgG in blocking buffer in the dark for 1 h at 37°C. The coverslips were washed three times with PBS and inverted onto glass slides with a drop of SlowFade solution and sealed with acrylic nail polish. One μm Z plane images were captured using an Apotome optical sectioning device. LAMP1 (red) and filipin (green) images were captured using a filter set consisting of 546 nm excitation, 580 nm dichroic mirror, 590 nm emission, and 365 nm excitation, 395 nm dichroic mirror, 420 nm long pass emission, respectively.

In the second procedure cultures were first incubated with a lysine-fixable polymer of 10,000 MW dextran conjugated to tetramethylrhodamine (D10K-TMR). This incubation was followed by a chase period, and an assessment of whether D10K-TMR fluorescence colocalized to punctate areas that also reacted with filipin or antibodies to LAMP1. D10K-TMR was prepared as a stock solution in PBS. On the evening of the first day after plating, cultures were incubated overnight with 0.1 mg/ml D10K-TMR in complete medium. Cultures were washed the following morning 3x with complete medium and then incubated an additional 8 h in complete medium ± 1 μM U18666A. Subsequently, cultures were washed 3x with PBS and fixed for 30 min with 4% paraformaldehyde/PBS (w/w). Thereafter, cultures were incubated with either filipin or LAMP1 antibody, and imaged as described above. D10K-TMR fluorescence was detected using a filter set consisting of 546 nm excitation, 580 nm dichroic mirror, and a 590 nm long pass emission filter.

### Colocalization of Filipin and MitoTracker

Control or treated cultures were incubated with 200 nM MitoTracker Green FM for 5 min at 37°C in a $CO_2$ incubator. Cells were washed three times with PBS and fixed as described above. After washing the coverslips three times with PBS, the cells were incubated in the dark with filipin as described above. The coverslips were washed three times with PBS and inverted onto glass slides with a drop of SlowFade solution and sealed with acrylic nail polish. MitoTracker Green FM (red) images were captured using a filter set consisting of 450–490 nm excitation, 510 nm dichroic mirror, and 515–565 nm emission. Images of filipin fluorescence (green) were captured as described above.

### Cellular localization of NPe6

Cultures were incubated with nothing or 1 μM U18666A for ~22 h prior to being washed and refed with medium containing 33 μM NPe6. After ~2 h the cultures were incubated with 1.5 μM LysoSensor Green DND-189 (LSG) for 10–15 min before being washed, refed and imaged. Phase and fluorescence images were captured with a Nikon E600 fluorescence microscope equipped with a Photometrics SenSys CCD camera (Roper Scientific, Trenton, NJ) cooled to −40°C. LSG was imaged first (excitation 450–490 nm; emission > 520 nm; low pass 600 nm filter) followed by NPe6 imaging (excitation 400–440 nm; emission ≥ 590 nm). For the purposes of colocalization, LSG and NPe6 fluorescence images were assigned ‘green’ and ‘red’ colors, respectively.

### Detection of reduced and oxidized C11-BODIPY

A stock solution of C11-BODIPY$^{581/591}$ (C11) was prepared in ethanol. 1c1c7 cultures were incubated with 4 μM C11 for 1 h prior to being washed, refed and immediately imaged with a Nikon E600 fluorescence microscope. In protocols designed to colocalize LSG with C11 (no NPe6 present), 2 μM LSG was added 10 min prior to the processing of cultures for fluorescence microscopy. Red C11 fluorescence (reduced C11) was detected using 540–550 nm excitation and 600–660 nm emission. A 650 nm low pass filter was used to further restrict emission in order to eliminate any contribution of NPe6 emission (when it was present) to the observed C11-derived red fluorescence. Green C11 fluorescence (oxidized

C11) was detected using a filter cube that provided 450–490 nm excitation and ≥ 515 nm emission. A 550 low pass filter was used to further restrict emission.

### Statistical analyses

Per cell filipin fluorescence was determined using a fixed exposure time for all samples within a comparison set, and quantified as 'arbitrary fluorescence units' using Metamorph Software (Universal Imaging Corporation, Buckinghamshire, UK). Acridine orange stained punctate acidic vesicles observed in enlarged digital pictures of stained cultures were counted by eye. Filipin and AO per cell data were analyzed by one-way ANOVA and Tukey's Multiple Comparison test (Prism, Graphpad Software, San Diego, CA, USA). Differences between/among groups were scored as statistically significant if $P<0.05$.

## Results

### CAD effects on cell proliferation and non-esterified cholesterol/sterol contents

A defect in the NPC1 protein is responsible for lysosomal sterol accumulation in cell lines derived from Niemann-Pick Type C (NPC) patients [25,26]. This phenotypic property of NPC cells can be induced in other cell types by exposure to U18666A [24–27] and other lysosomotrophic CADs, including imipramine [24]. Exposure of murine hepatoma 1c1c7 cultures to 1 μM U18666A, 25 μM imipramine or 10 μM clozapine had little, if any effect, on cell proliferation over a 96 h treatment period (Fig. 1A). Trypan blue exclusion analyses indicated that none of these CADs, at the concentrations tested, were cytotoxic to 1c1c7 cells (data not shown).

Filipin is a fluorescent natural product with very high affinity for sterol molecules containing a free 3β-hydroxyl group [28]. Although it also interacts with some oxysterols, cholesterol esters, and phospholipids [29,30], it does so with markedly less affinity [29], and hence is commonly used to detect non-esterified cholesterol/sterols [26–29,31]. Filipin staining in non-treated 1c1c7 cultures was diffuse, with a few perinuclear punctate stained areas (Figs. 1B,D,E). Exposure to DMSO did not alter staining (Fig. 1B). However, concentration-dependent accumulation of filipin-stained, perinuclear punctate structures occurred within 22 h of treatment with 0.05 – 1.0 μM U18666A (Figs. 1B,C). The threshold at which increased punctate filipin staining could be visually observed consistently was 0.05 μM. The CADs imipramine and clozapine also induced concentration-dependent accumulation of filipin-stained, perinuclear punctate structures (Fig. 1D). The thresholds at which increased punctate filipin staining could be visually observed consistently following ~24 h of treatment with imipramine or clozapine were 1 μM and 5 μM, respectively.

The kinetics of non-esterified cholesterol/sterol redistribution following CAD treatment are presented in Fig. 1E. Increased punctate filipin staining was observed within 8 and 16 h of U18666A and imipramine treatment, respectively. Thereafter, the intensity of punctate staining continued to increase over the 24 h experimental time period with both CADs (Fig. 1E). Extended monitoring through 96 h indicated that the intensities of filipin-stained punctate structures continued to increase with exposure time to U18666A or imipramine without obvious cytotoxicity (data not presented).

### Filipin staining colocalizes to late endosomes/lysosomes, but not mitochondria, in U18666A-treated 1c1c7 cultures

We employed two approaches to characterize the identity of the filipin-stained punctate structures. Our first approach employed a two-step protocol to co-localize late endosomes/lysosomes and filipin-stained structures. The fluorescent polymer dextran-10,000 tetramethylrhodamine (D10K-TMR) enters cells by endocytosis, and eventually resides in

lysosomes following a sufficient chase period [27]. Overnight loading of 1c1c7 cultures with D10K-TMR, followed by an 8 h chase with fresh medium, resulted in extensive co-localization of D10K-TMR with LAMP1-positive structures (Fig. 2A, top row). Similar results were obtained if cultures were supplemented with 1 μM U18666A at the beginning of the chase period (Fig. 2A, bottom row). Hence, in this protocol much of the endocytosed D10K-TMR trafficked to late endosomes/lysosomes.

In non-treated cultures there was limited colocalization of filipin and D10K-TMR (Fig. 2B, top row). In contrast, filipin staining was very punctate in U18666A-treated cultures, and extensively co-localized with D10K-TMR fluorescence (Fig. 2B, bottom row). Given the co-localization of D10K-TMR with both LAMP1 and filipin-stained punctate structures, it appears that a majority of the filipin-stained punctate structures in U18666A-treated cultures represent late endosomes/lysosomes.

Experiments identical to those reported in Figs. 2A and B were also performed with imipramine. Cultures treated with 12.5 μM imipramine also exhibited extensive punctate LAMP1 and filipin co-localization with D10K-TMR (data not presented).

In our second approach to identify filipin-stained punctate structures we colocalized filipin staining with the late endosome/lysosome marker LAMP1. Control cultures exhibited diffuse filipin staining with a few punctate spots that co-stained for LAMP1 and filipin (Fig. 2C, top row). Conversely, cultures treated with U18666A for 24 h exhibited increased numbers of filipin- and LAMP1-co-stained perinuclear punctate structures (Fig. 2C, bottom row). Furthermore, relative to control cultures, the co-stained punctate structures were much larger in U18666A-treated cells. Indeed, the U18666A-derived structures were of sufficient size to clearly exhibit LAMP1 staining of specifically the membrane (Fig. 2C, bottom row).

A recent study suggests that U18666A also promotes non-esterified cholesterol/sterol accumulation in mitochondria [32]. Non-treated and U18666A-treated 1c1c7 cells exhibited extensive organelle fluorescence after incubation with the mitochondrial stain MitoTracker Green FM (Fig. 2D). However, MitoTracker Green FM and filipin fluorescence did not colocalize in either non-treated or U18666A-treated cultures (Fig. 2D).

### CAD inhibition of LMP initiated by photoirradiation of NPe6-sensitized cultures

The fluorescent dye acridine orange (AO) diffuses into late endosomes/lysosomes, and fluoresces orange-red in acidic environments. Loss of punctate orange-red AO fluorescence is commonly used to monitor LMP. We [7] and others [33] previously reported that the photosensitizer NPe6 localizes to late endosomes/lysosomes, and that photoirradiation of NPe6-sensitized 1c1c7 cultures results in LMP and apoptosis [7,21]. Indeed, punctate AO orange-red fluorescence was eliminated in 1c1c7 cultures first sensitized with NPe6, and then photoirradiated for either 65 or 80 s (Figs. 3A top row, B). This effect required combinational NPe6 + light treatment since neither light alone, nor 33 μM NPe6 alone, markedly affected punctate AO fluorescence in 1c1c7 cultures [7,21] (see also Fig. 4D). Treatment with 1 μM U18666A or 12.5 μM imipramine appeared to intensify AO fluorescence (Fig. 3A, second and third row, respectively). Pretreatment with either CAD also suppressed NPe6 PDT-induced losses of AO fluorescent punctate structures (Figs. 3A,B).

As a complement to the AO-staining studies, we also monitored the colocalization of LAMP1 with the lysosomal protease cathepsin D (Supplementary Fig. 1). These two proteins exhibited extensive colocalization in non-treated and U18666A-treated cultures, as indicated by the very high percentage of punctate structures exhibiting yellow fluorescence (due to colocalization of ‘red’ Lamp1 positive structures and ‘green’ cathepsin D positive

structures). This colocalization was partially lost in photoirradiated, NPe6-sensitized cultures, as indicated by the loss of orange-yellow spots, and a reciprocal increase in red (LAMP1 positive) punctate spots (Supplementary Fig. 1, third row). Pretreatment with U18666A suppressed NPe6 PDT-induced losses of LAMP1 and cathepsin D colocalization (Supplementary Fig. 1, fourth row).

Two approaches were employed to determine if lysosomal non-esterified cholesterol/sterol accumulations were responsible for U18666A-mediated suppression of NPe6 PDT-induced LMP. First, we took advantage of our finding that the intensity of filipin-stained punctate structures is proportional to U18666A concentration over the range 0.05 – 1 μM (Figs. 1B and C). Figs. 3C and D, in conjunction with Figs. 1B and C, show that the extent of punctate AO fluorescence after NPe6 PDT directly correlates with the intensity of filipin staining at the time of irradiation. No protection (*i.e*., as indicated by loss of AO punctate fluorescence) was observed with a concentration of U18666A (*i.e*., 10 nM) insufficient to increase punctate filipin staining. Thereafter, the degree of protection increased with increasing U18666A concentration.

The second approach exploited the finding that the effects of U18666A on non-esterified cholesterol/sterol accumulation were reversible. Specifically, punctate filipin staining decreased markedly within 24 h of refeeding U18666A-treated cultures with CAD-free medium (Fig. 4A). Filipin staining continued to decrease over time. After 96 h of washout filipin staining approached the levels observed in non-treated cultures (Fig. 4A). This decrease was not accompanied by dramatic changes in punctate AO fluorescence (Fig. 4B). However, it was paralleled by increased sensitivity to PDT-induced LMP (Fig. 4C). Specifically, in PDT-treated cultures, minor and dramatic losses of punctate AO fluorescence were observed within 48 h and 96 h of washout, respectively. Indeed, cultures having undergone a 96 h washout were just as susceptible to NPe6 PDT-induced LMP as were cultures that had never been exposed to U18666A (compare 96 h PDT panel in Fig. 4C with PDT panel in Fig. 4D).

## CAD inhibition of NPe6-PDT induced apoptosis

We previously reported that 1c1c7 cultures undergo apoptosis following NPe6 PDT-induced LMP [7,21]. Pretreatment with concentrations of U18666A (1 μM) or imipramine (12.5 μM) sufficient to suppress NPe6 PDT- induced LMP also inhibited the activation of DEVDase, an indicator of caspase-3/7 activity (Figs. 5A,B). Western blot analyses confirmed that preincubation with U18666A or imipramine suppressed pro-caspase-9 and pro-caspase-3 processing (Fig. 5D). Pretreatment with 10 μM clozapine, a concentration sufficient to induce non-esterified cholesterol/sterol accumulation in lysosomes, also suppressed NPe6 PDT-induced DEVDase activation (Fig. 5C) and pro-caspase-9/3 processing (Fig. 5D). Concentration-response studies exhibited an inverse relationship between CAD-induced lysosomal accumulation of sterols and susceptibility to NPe6 PDT-induced DEVDase activation (Figs. 5A–C).

## Effects of CADs on NPe6 intracellular location

The induction of LMP in NPe6 PDT protocols requires that the photosensitizer accumulate in the lysosomes. In agreement with previous studies [7,33], NPe6 extensively colocalized in control cultures with the acidic organelle fluorescent probe LysoSensor Green (Supplementary Fig. 2). Extensive colocalization was also observed in U18666A-treated cultures (Supplementary Fig. 2). Indeed, both LysoSensor Green and NPe6 fluorescence were brighter in U18666A-treated cultures. This enhanced fluorescence is consistent with the increased AO staining seen in U18666A-treated cultures (Fig. 3A). The colocalization studies are significant because they document that the photosensitizer is associated with the

target organelles, and capable of being photo-activated by illumination. Hence, U18666A-mediated suppression of NPe6 PDT-induced LMP is not due to an effect on photosensitizer loading.

### UA18666A-mediated suppression of PDT-induced oxidation of C11-BODIPY

C11-BODIPY$^{581/591}$ (C11) is a fluorescent fatty acid analog that is incorporated into the membranes of organelles of cultured cells [34–36]. Following excitation at 488 nm, C11 yields red fluorescence. However, C11 fluoresces green upon oxidation of its diene linker and loss of a phenyl moiety. Hence, C11 is commonly used as a reporter molecule for assessing membrane lipid peroxidation [34–36]. 1c1c7 cultures incubated with C11 for 1 h exhibited intense perinuclear red fluorescence, but no green fluorescence (Fig. 6A). Given the absence of green fluorescence, we attempted to determine if C11 labeled endosomes/lysosomes by cotreating cultures with LSG (Fig. 6B). Cultures treated with LSG yielded green punctate fluorescence. Overlay of C11 and LSG fluorescence patterns yielded punctate orange/yellow spots indicative of colocalization. Hence, as had been reported for rat-1 fibroblasts [35], C11 labeled late endosomes/lysosomes in 1c1c7 cultures.

Photoirradiation of NPe6-sensitized cultures for 60 s, a period sufficient to induce LMP (as assessed by AO staining), resulted in the appearance of punctate green C11 fluorescence, and the corresponding loss of red fluorescence in the areas that fluoresced green (Fig. 6C). Hence, NPe6 PDT induced the oxidation of C11. Exposure of cultures to UA18666A for ~20 h prior to the addition of C11 did not cause a shift in C11 fluorescence from red to green (Fig. 6D). However, U18666A pretreatment strongly suppressed NPe6 PDT-induced C11 oxidation (Fig. 6E), as indicated by the absence of green fluorescence following photoirradiation.

### PDT-induced cholesterol oxidation

One possible explanation for the inhibitory effect of U18666A pretreatment on C11 oxidation in PDT protocols is that cholesterol functions as a more susceptible target to the generated oxidant. To assess this possibility we took advantage of the report that oxidized cholesterol yields less fluorescence with filipin than does the non-oxidized sterol [29]. Photoirradiation of U18666A-pretreated cultures for either 60 or 120 s reduced subsequent staining with filipin (Fig. 7A). The degree to which staining was reduced was influenced by lysosomal sterol content. Whereas 60 s of photoirradiation markedly reduced filipin staining in cultures pretreated with 0.1 μM U18666A, staining was less affected in cultures treated with 0.75 μM U18666A. More extensive and quantitative analyses indicated a progressive decline in filipin staining with increasing light dose in cultures pretreated with either U18666A concentration (Fig. 7B). However, the overall extent of filipin staining loss was greater in 0.1 μM U18666A-treated cultures (*i.e.*, 70% loss versus 50% loss after 120 s of photoirradiation).

### U18666A-mediated suppression of $H_2O_2$-induced LMP and DEVDase activation

Brunk and colleagues reported that exogenously added $H_2O_2$ induces LMP in several types of cultured cells [4,5]. Preliminary studies indicated that a reproducible apoptotic response could be induced in 1c1c7 cultures by exposure to 100 – 400 μM $H_2O_2$. Necrosis was also observed at the higher end of this range. Figure 8A presents analyses of $H_2O_2$-induced DEVDase activation over the range 100 – 200 μM. DEVDase activities were maximally increased ~5-, 15- and 20-fold above background by 100, 150 and 200 μM $H_2O_2$, respectively. Pretreatment with U18666A suppressed $H_2O_2$-mediated DEVDase activation (Fig. 8B). This suppression was concentration-dependent and correlated directly with U18666A-mediated accumulation of non-esterified cholesterol/sterols (compare Figs. 1B and 8B).

A pro-apoptotic concentration of $H_2O_2$ also induced LMP, as indicated by the loss of punctate AO fluorescence (Fig. 8C). Specifically, markedly less punctate AO fluorescence was observed in 1c1c7 cultures following 4 or 6 h of $H_2O_2$ exposure. This loss of punctate AO staining was prevented by pretreating cultures with 1 μM U18666A for 20 h prior to peroxide addition (Fig. 8C).

### Specificity of the anti-apoptotic properties of U18666A and imipramine

In the above studies U18666A and imipramine inhibited the proapoptotic activities of agents that caused LMP. At issue is whether the CADs would afford protection against toxicants that initiate apoptosis by mechanisms independent of LMP. To address this question we surveyed the effects of U18666A and imipramine on the induction of apoptosis by HA14-1, thapsigargin and staurosporine. These agents have diverse mechanisms of action, and do not initiate apoptosis in 1c1c7 cultures via the induction of LMP [14] (Reiners, unpublished data). HA14-1 is a small molecule inhibitor of members of the anti-apoptotic Bcl-2 family, as well as an uncoupler of mitochondrial respiration [37]. Twenty five μM HA14-1 caused > 100-fold activation of DEVDase within an h of treatment (Figs. 9A,D). Pretreatment with either 1 μM U18666A or 12.5 μM imipramine had little effect on either the kinetics or extent of DEVDase activation (Figs. 9A,D). The sarcoplasmic endoplasmic reticulum ATP $Ca^{2+}$ pump inhibitor thapsigargin, and the broad spectrum kinase inhibitor staurosporine, induced a ≥ 50-fold activation of DEVDase (Figs. 9B,C,E,F). Pretreatment with U18666A (Figs. 9B,C) or imipramine (Figs. 9E,F) did not alter the kinetics or extent of DEVDase activation induced by either pro-apoptotic agent.

## Discussion

The current study demonstrates that lysosomal non-esterified cholesterol/sterol content modulates the induction of LMP by reactive oxygen species (ROS). Specifically, susceptibility to the induction of LMP by the singlet oxygen generated in the NPe6 PDT protocol, or by exogenously added $H_2O_2$, was inversely related to lysosomal non-esterified cholesterol/sterol content. The critical oxidants in these studies were most likely generated within the organelle itself. Lysosomes accumulate iron, and the inclusion of an iron chelator suppresses $H_2O_2$-induced LMP in whole cells and isolated lysosomes [5]. Presumably, intra-organelle Fenton reaction-derived hydroxyl radicals are responsible for $H_2O_2$-induced LMP. As for NPe6, the studies presented in Supplementary Fig. 2 document the endosomal/lysosomal location of the sensitizer. The singlet oxygen generated following photoactivation is exceptionally reactive, and reacts with suitable targets within its immediate vicinity [38,39].

The exact mechanism(s) by which $H_2O_2$ and NPe6 PDT induce LMP is not known. Given the strong oxidants involved, and their presumed intra-organelle generation, it is conceivable that LMP is due to oxidant-induced damage to lysosomal membrane lipids and proteins. Girotti [40] has demonstrated that membrane cholesterol/sterols are readily oxidized by exposure to singlet oxygen or hydroxyl radicals. Furthermore, the incorporation of cholesterol into liposomes has been reported to suppress ROS-induced lipid peroxidation [41,42]. In the current study, lysosomal filipin-staining intensities were inversely related to the light dose used for NPe6 PDT. Since oxidized cholesterol exhibits reduced filipin staining compared to the non-oxidized sterol [29], our data are consistent with lysosomal cholesterol being oxidized by the reactive species generated following photoactivation of intra-lysosomal NPe6. Importantly, the NPe6 PDT-induced oxidation of late endosome/lysosomal cholesterol in U18666A-treated cultures was paralleled by the suppression of PDT-induced organelle-associated C11 oxidation (see Fig. 6). Although we did not unequivocally demonstrate that the C11 oxidation observed in NPe6 PDT–treated cultures occurred in endosomes/lysosomes, there is good reason to assume so. Specifically, NPe6

accumulates primarily in late endosomes/lysosomes [7,33and Supplementary Fig. 2], and the singlet oxygen generated upon photoirradiation is exceptionally reactive and has a very limited diffusion radius [38,39]. Presumably, by being an available and susceptible target, elevated lysosomal cholesterol content may lessen the probability of damage to membrane lipids and/or proteins more relevant to processes involved in LMP.

Although our current studies are consistent with the protective effects of lysosomal cholesterol being mediated by its being an alternative target and functioning as an antioxidant, the sterol may afford protection by alternative mechanisms. For example, increased cholesterol content may alter the architecture of the lysosomal membrane such that it becomes less susceptible to the effects of oxidants. Indeed, cholesterol is a major modulator of membrane fluidity. Increasing membrane cholesterol content alters phospholipid orientation and packing, resulting in more rigid, less fluid membranes [43]. Such changes may influence the recruitment of proteins to the organelle that enhance membrane stability, such as members of the Hsp70 family. Hsp70 over-expression and knockdown studies indicated that $H_2O_2$ destabilization of lysosomal membranes in HeLa cultures is inversely related to cellular/lysosomal Hsp70 content [9,12].

LMP may be achieved by mechanisms other than oxidant-induced membrane rupture. Recent studies suggest that LMP is facilitated by the association of specific proteins with lysosomes [18–20]. The adaptor protein LAPF translocates to lysosomes following exposure to TNFα, whereupon it recruits and binds phosphorylated p53 (Ser15/18) [20]. Knockdown/silencing of either LAPF or p53 expression suppressed TNF-induced LMP [20]. Similarly, treatment of cultured cholangiocarcinoma cell lines with TRAIL results in the association of ‘activated’ Bax with lysosomes [15]. Knockdown of Bax expression, or interruption of the processes mediating Bax association with the lysosomes, suppressed TRAIL-induced LMP [15]. Although speculative, lysosomal Bax and LAPF/p53 complexes may form pores through which the luminal contents of lysosomes pass. At issue is whether lysosomal non-esterified cholesterol/sterol accumulation would be protective in the above models.

Presumably, U18666A and imipramine inhibit the induction of apoptosis by $H_2O_2$ and NPe6 PDT in our studies, in part or whole, because of their abilities to suppress LMP. Indeed, concentration response studies demonstrated that the degree to which the CADs suppressed the induction of apoptosis and LMP were strongly correlated. Although a recent study suggests that U18666A also promotes accumulation of non-esterified cholesterol/sterols in mitochondria [32], which could be a confounder to the interpretation of our data, such accumulations were not observed in our studies (see Fig. 2D). Furthermore, U18666A did not inhibit the activation of procaspases by agents known to activate the intrinsic apoptotic pathway (*i.e*., HA14-1, staurosporine), or the ER stress pathway (*i.e*., thapsigargin). Hence, the anti-apoptotic effects of U18666A in our model appear to be restricted to agents/protocols causing oxidant-induced LMP.

Schafer *et al.* [44] reported that HT22 hippocampal cells conditioned to grow in medium containing sublethal doses of $H_2O_2$ develop resistance to the peroxide, as well as other oxidants. However, these cells were as susceptible as the parental line to non-oxidant toxicants. A recent study by Clement *et al.* [45] indicates that lysosomes of oxidant-resistant HT22 cells have elevated non-esterified cholesterol/sterol contents. Given these findings and our current studies, it is conceivable that lysosomal cholesterol accumulation maybe an adaptive response to chronic oxidant-induced stress.

Lysosomal accumulation of non-esterified cholesterol/sterols occurs as a consequence of several diseases, of which NPC is the best characterized [24–26,46]. NPC is one of approximately 4 dozen inherited metabolic disorders collectively referred to as lysosomal

storage diseases [46]. Filipin staining of cell lines generated from patients with lysosomal storage disease indicate that most, but not all of the disorders, support lysosomal accumulations of non-esterified cholesterol/sterols [47]. We anticipate that cells derived from such patients, that exhibit enhanced lysosomal filipin staining, would be resistant to some forms of oxidant-induced apoptosis. This is the case with Niemann-Pick type A cells. These cells are deficient in acidic sphingomyelinase, accumulate non-esterified cholesterol [47]. and are more resistant than their normal counterparts to the pro-apoptotic effects of $H_2O_2$ [48].

Phospholipidosis is a lipid storage disorder characterized by lysosomal accumulation of phospholipids. CADs are small lysosomotrophic chemicals containing both a hydrophobic ring structure and a hydrophilic side chain with a charged cationic amine group. Dozens of CADs have been identified which cause phospholipidosis [49,50]. Although the classic phenotypic marker of phospholipidosis is lysosomal accumulation of lamellar bodies, filipin staining suggests that CAD-treated cells accumulate non-esterified cholesterol/sterols in their late endosomes/lysosomes [24,26,27]. Indeed, in our studies the CADs U18666A, imipramine and clozapine all induced lysosomal non-esterified cholesterol/sterol accumulation at non-cytostatic, and non-toxic concentrations. All three also protected against the induction of LMP and apoptosis by NPe6 PDT at concentrations sufficient to induce lysosomal non-esterified cholesterol accumulation. We have also examined the CADs amitriptyline, fluoxetine, amiodarone and chlorpromazine. These agents also induced lysosomal non-esterified cholesterol/sterol accumulation in 1c1c7 cultures. However, we did not pursue additional studies with these agents since cholesterol accumulation occurred with concentrations that either exhibited some cytotoxicity, or that suppressed NPe6 loading (Reiners, unpublished studies). Nevertheless, CADs are commonly used in human medicine as estrogen receptor antagonists (Tamoxifen), anti-psychotics (clozapine), anti-depressants (imipramine, amitriptyline, fluoxetine), anti-arrythmics (amiodarone), anti-bacterials (azithromycin) and anti-malarials (chloroquine).

In summary, the current study demonstrates that lysosomal accumulation of non-esterified cholesterol/sterols inhibits ROS-mediated LMP, and the ensuing apoptotic response initiated as a consequence of LMP. These findings are significant because lysosomal accumulation of non-esterified cholesterol/sterols is a phenotypic characteristic of several diseases and pathological conditions. In addition, it may be a consequence of an adaptive response to chronic oxidative stress. Finally, a large number of agents cause LMP, including several therapeutic pharmaceuticals. Appreciation that lysosomal cholesterol content can influence susceptibility to oxidant-induce LMP may facilitate better-designed therapeutic protocols.

## Supplementary Material

Refer to Web version on PubMed Central for supplementary material.

## Acknowledgments

This work was supported in part by National Institutes of Health grants ES09392 and CA233378. M. Kleinman is a predoctoral trainee who was supported by National Institutes of Health grant T32 ES01216.

## Abbreviations

| | |
|---|---|
| **AhR** | aryl hydrocarbon receptor |
| **AO** | acridine orange |
| **Ac-DEVD-AMC** | acetyl-Asp-Glu-Val-Asp-7-amino-4-methylcoumarin |

| | |
|---|---|
| **AMC** | 7-amino-4-methylcoumarin |
| **C11** | C11-BODIPY$^{581/591}$ or 4,4-difluoro-5-(4-phenyl-1,3,butadienyl)-4-bora-3a,4a-diaza-*s*-indacene-3-undecanoic acid |
| **CAD** | cationic amphiphilic drug |
| **CZP** | clozapine |
| **D10K-TMR** | dextran-10,000 tetramethylrhodamine |
| **HA14-1** | ethyl 2-amino-6-bromo-4-(1-cyano-2-ethoxy-2-oxoethyl)-4H-chromene-3-carboxylate |
| **IPM** | imipramine |
| **LAMP1** | lysosomal-associated membrane protein 1 |
| **LAPF** | lysosome-associated apoptosis-inducing protein containing the pleckstrin homology and FYVE domains |
| **LMP** | lysosomal membrane permeability |
| **LSG** | LysoSensor Green |
| **MTG** | MitoTracker Green |
| **NPC** | Niemann-Pick Type C |
| **NPe6** | mono-L-aspartyl chlorin e6 |
| **PDT** | photodynamic treatment |
| **NT** | not treated |
| **ROS** | reactive oxygen species |
| **UA** | U18666A or 3-β-[(2-diethyl-amino) ethoxy]androst-5-en-17-one |

## References


1. Johansson A-C, Appelqvist H, Nilsson C, Kagedal K, Roberg K, Öllinger K. Regulation of apoptosis-associated lysosomal membrane permeabilization. Apoptosis. 2010; 15:478–484.
2. Guicciardi ME, Leist M, Gores GJ. Lysosomes in cell death. Oncogene. 2004; 23:2881–2890. [PubMed: 15077151]
3. Kirkegaard T, Jäättelä M. Lysosomal involvement in cell death and cancer. Biochim. Biophys. Acta. 2009; 1793:746–754. [PubMed: 18948147]
4. Dare E, Li W, Zhivotorsky B, Yuan S, Ceccatelli S. Methyl mercury and $H_2O_2$ provoke lysosomal damage in human astrocytoma D384 cells followed by apoptosis. Free Radic. Biol. Med. 2001; 30:1347–1356. [PubMed: 11390179]
5. Kurtz T, Gustafsson B, Brunk UT. Intralysosomal iron chelation protects against oxidative stress-induced cellular damage. FEBS J. 2006; 273:3106–3117. [PubMed: 16762036]
6. Roberg K, Johansson U, Öllinger K. Lysosomal release of cathepsin D precedes relocation of cytochrome c and loss of mitochondrial transmembrane potential during apoptosis induced by oxidative stress. Free Radic. Biol. Med. 1999; 27:1228–1237. [PubMed: 10641715]
7. Reiners JJ Jr, Caruso JA, Mathieu P, Chelladurai B, Yin X-M, Kessel D. Release of cytochrome c and activation of pro-caspase-9 following lysosomal photodamage involves Bid cleavage. Cell Death Differ. 2002; 9:934–944. [PubMed: 12181744]
8. Berg K, Moan J. Lysosomes as photochemical targets. Int. J. Cancer. 1994; 59:814–822. [PubMed: 7989124]

9. Bivik C, Rosdahl L, Öllinger K. Hsp70 protects against UVB induced apoptosis by preventing release of cathepsins and cytochrome c in human melanocytes. Carcinogenesis. 2007; 28:537–544. [PubMed: 16950797]
10. Paquet C, Sane AT, Beauchemin M, Bertrand R. Caspase-and mitochondrial dysfunction-dependent mechanisms of lysosomal leakage and cathepsin B activation in DNA-damage-induced apoptosis. Leukemia. 2005; 19:784–791. [PubMed: 15759029]
11. Emert-Sedlak L, Shangary S, Rabinovitz A, Miranda MB, Delach SM, Johnson DE. Involvement of cathepsin D in chemotherapy-induced cytochrome c release, caspase activation, and cell death. Mol. Cancer Ther. 2005; 4:733–742. [PubMed: 15897237]
12. Gyrd-Hansen M, Nylandsted J, Jäättelä M. Heat shock protein 70 promotes cancer cell viability by safeguarding lysosomal integrity. Cell Cycle. 2004; 12:1484–1485. [PubMed: 15539949]
13. Fehrenbacher N, Bastholm L, Kirkegaard-Sorensen T, Rafn B, Bottzauw T, Nielsen C, Weber E, Shirasawa S, Kallunki T, Jäättelä M. Sensitization to the lysosomal cell death pathway by oncogene-induced down regulation of lysosome-associated membrane proteins 1 and 2. Cancer Res. 2008; 68:6623–6633. [PubMed: 18701486]
14. Caruso JA, Mathieu PA, Joiakim A, Zhang H, Reiners JJ Jr. Aryl hydrocarbon receptor modulation of TNFα-induced apoptosis and lysosomal disruption in a hepatoma model that is caspase-8 independent. J. Biol. Chem. 2006; 281:10954–10967. [PubMed: 16446372]
15. Werneburg NW, Guicciardi ME, Bronk SF, Kaufmann SH, Gores GJ. Tumor necrosis factor-related apoptosis-inducing ligand activates a lysosomal pathway of apoptosis that is regulated by Bcl-2 proteins. J. Biol. Chem. 2007; 282:28960–28970. [PubMed: 17686764]
16. Nagaraj NS, Vigneswaran N, Zacharias W. Hypoxia inhibits TRAIL-induced tumor cell apoptosis: involvement of lysosomal cathepsins. Apoptosis. 2007; 12:125–139. [PubMed: 17136492]
17. Berndtsson M, Beaujouin M, Rickardson L, Havelka AM, Larsson R, Westman J, Liaudet-Coopman E, Linder S. Induction of the lysosomal apoptosis pathway by inhibitors of the ubiquitin-proteasome system. Int. J. Cancer. 2009; 124:1463–1469. [PubMed: 19089926]
18. Kågedal K, Johansson AC, Johansson U, Heimlich G, Roberg K, Wang NS, Jurgensmeier JM, Öllinger K. Lysosomal membrane permeabilization during apoptosis-involvement of Bax? Int. J. Exp. Pathol. 2005; 86:309–321. [PubMed: 16191103]
19. Yuan X-M, Li W, Dalen H, Lotem J, Kama K, Sachs L, Brunk UT. Lysosomal destabilization in p53-induced apoptosis. Proc. Natl. Acad. Sci. USA. 2002; 99:6286–6291. [PubMed: 11959917]
20. Li N, Zheng Y, Chen W, Wang C, Liu X, He W, Xu H, Cao X. Adaptor protein LAPF recruits phosphorylated p53 to lysosomes and triggers lysosomal destabilization in apoptosis. Cancer Res. 2007; 67:11176–11185. [PubMed: 18056442]
21. Caruso JA, Mathieu PA, Joiakim A, Leeson B, Kessel D, Sloane BF, Reiners JJ Jr. Differential susceptibilities of murine hepatoma 1c1c7 and Tao cells to the lysosomal photosensitizer NPe6: Influence of aryl hydrocarbon receptor on lysosomal fragility and protease contents. Mol. Pharmacol. 2004; 65:1016–1028. [PubMed: 15044632]
22. Hao SJ, Hou JF, Jiang N, Zhang GJ. Loss of membrane cholesterol affects lysosomal osmotic stability. Gen. Physiol. Biophys. 2008; 27:278–283. [PubMed: 19202201]
23. Yang L, Zhang GJ, Zhong Y-G, Zheng Y-Z. Influence of membrane fluidity modifiers on lysosomal osmotic sensitivity. Cell Biol. Internat. 2000; 24:699–704.
24. Lange Y, Ye J, Steck TL. Circulation of cholesterol between lysosomes and the plasma membrane. J. Biol. Chem. 1998; 273:18915–18922. [PubMed: 9668068]
25. Lange Y, Ye J, Rigney M, Steck T. Cholesterol movement in Niemann-Pick Type C cells and in cells treated with amphiphiles. J. Biol. Chem. 2000; 275:17468–17475. [PubMed: 10751394]
26. Cenedella RJ. Cholesterol synthesis inhibitor U18666A and the role of sterol metabolism and trafficking in numerous pathophysiological processes. Lipids. 2009; 44:477–487. [PubMed: 19440746]
27. Lebrand C, Corti M, Goodson H, Cosson P, Cavalli V, Mayran N, Faure J, Gruenberg J. Late endosome motility depends on lipids via the small GTPase Rab7. EMBO J. 2002; 21:1289–1300. [PubMed: 11889035]
28. Gimpl G, Gehrig-Burger K. Cholesterol reporter molecules. Biosci. Rep. 2007; 27:335–358. [PubMed: 17668316]

29. Smejkal GB, Hoppe G, Hoff HF. Filipin as a fluorescent probe of liproprotein-derived sterols on thin-layer chromatograms. Anal. Biochem. 1996; 239:115–117. [PubMed: 8660636]
30. Milhaud J. Permeabilizing action of filipin III on model membranes through a filipin-phospholipid binding. Biochim. Biophys. Acta. 1992; 1105:307–318. [PubMed: 1375101]
31. Issandou M, Guillard R, Boullay A-B, Linhart V, Lopez-Perez E. Up-regulation of low density lipoprotein receptor in human hepatocytes is induced by sequestration of free cholesterol in the endosomal/lysosomal compartment. Biochem. Pharmacol. 2004; 67:2281–2289. [PubMed: 15163559]
32. Lucken-Ardjomande S, Montessuit S, Martinou J-C. Bax activation and stress-induced apoptosis delayed by the accumulation of cholesterol in mitochondrial membranes. Cell Death Differ. 2008; 15:484–493. [PubMed: 18084240]
33. Roberts WG, Liaw LH, Bern MW. In vitro photosensitization II. An electron microscopy study of cellular destruction with mono-L-aspartyl chlorin e6 and photofrin II. Lasers Surg. Med. 1989; 9:102–108. [PubMed: 2523992]
34. Pap EHW, Drummen GPC, Winter VJ, Kooij TWA, Rijken P, Wirtz KWA, Op Den Kamp JAF, Hage WJ, Post JA. Ratio-fluorescence microscopy of lipid oxidation in living cells using C11-BODIPY$^{581/591}$. FEBS Lett. 1999; 453:278–282. [PubMed: 10405160]
35. Drummen GP, van Liebergen LC, Op den Kamp JA, Post JA. C11-BODIPY (581/591), an oxidation-sensitive fluorescent lipid peroxidation probe: (micro)spectroscopic characterization and validation of methodology. Free Radic. Biol. Med. 2002; 33:473–490. [PubMed: 12160930]
36. MacDonald ML, Murray IVJ, Axelsen PH. Mass spectrometric analysis demonstrates that BODIPY 581/599 C11 overestimates and inhibits oxidative lipid damage. Free Radic. Biol. Med. 2007; 42:1392–1397. [PubMed: 17395012]
37. Milanesi E, Costantini P, Gambalunga A, Colonna R, Petronilli V, Cabrelle A, Semenzato G, Cesura AM, Pinard E, Bernardi P. The mitochondrial effects of small organic ligands of BCL-2: sensitization of BCL-2 overexpressing cells to apoptosis by pyrimidine-2,4,6-trione derivative. J. Biol. Chem. 2006; 281:10066–10072. [PubMed: 16481323]
38. Moan J, Berg K. The photodegradation of porphyrins in cells can be used to estimate the lifetime of singlet oxygen. Photochem. Photobiol. 1991; 53:549–553. [PubMed: 1830395]
39. Dysart JS, Patterson MS. Characterization of Photofrin photobleaching for singlet oxygen dose estimation during photodynamic therapy of MLL cells in vitro. Phys. Med. Biol. 2005; 50:2597–2626. [PubMed: 15901957]
40. Girotti AW. Photosensitized oxidation of membrane lipids: reaction pathways, cytotoxic effects, and cytoprotective mechanisms. J. Photochem. Photobiol. 2001; 63:103–113.
41. Wiseman H, Cannon M, Arnstein HRV, Halliwell B. Mechanism of inhibition of lipid peroxidation by tamoxifen and 4-hydroxytamoxifen introduced into liposomes. FEBS Lett. 1990; 274:107–110. [PubMed: 2253763]
42. Wiseman H, Smith C, Halliwell B, Cannon M, Arnstein HRV, Lennard MS. Droloxifene (3-hydroxytamoxifen) has membrane antioxidant ability: potential relevance to its mechanism of therapeutic action in breast cancer. Cancer Letters. 1992; 66:61–68. [PubMed: 1451097]
43. Ridway ND. Interactions between metabolism and intracellular distribution of cholesterol and sphingomyelin. Biochim. Biophys. Acta. 2000; 1484:129–141. [PubMed: 10760463]
44. Schafer M, Goodenough S, Moosemann B, Behl C. Inhibition of glycogen synthase kinase 3-beta is involved in the resistance to oxidative stress in neuronal HT22 cells. Brain Res. 2004; 275:38104–38110.
45. Clement AB, Gamerdinger M, Tamboli IY, Lutjohann D, Walter J, Greeve I, Gimpl G, Behl C. Adaptation of neuronal cells to chronic oxidative stress is associated with altered cholesterol and sphingolipid homeostasis and lysosomal function. J. Neurochem. 2009; 111:669–682. [PubMed: 19712059]
46. Winchester B, Vellodi A, Young E. The molecular basis of lysosomal storage diseases and their treatment. Biochem. Soc. Trans. 2000; 28:150–154. [PubMed: 10816117]
47. Pagano RE, Puri V, Dominguez M, Marks DL. Membrane traffic in sphingolipid storage diseases. Traffic. 2000; 1:807–815. [PubMed: 11208071]

48. Komatsu M, Takahashi T, Abe T, Takahashi I, Ida H, Takada G. Evidence for the association of ultraviolet-C and $H_2O_2$-induced apoptosis with acid sphingomyelinase activation. Biochim. Biophys. Acta. 2001; 1533:47–54. [PubMed: 11514235]

49. Halliwell WH. Cationic amphiphilic drug-induced phospholipidosis. Toxicol. Path. 1997; 25:53–60. [PubMed: 9061852]

50. Reasor MJ, Kacew S. Drug-induced phospholipidosis: are there functional consequences? Exp. Biol. Med. 2001; 226:825–830.

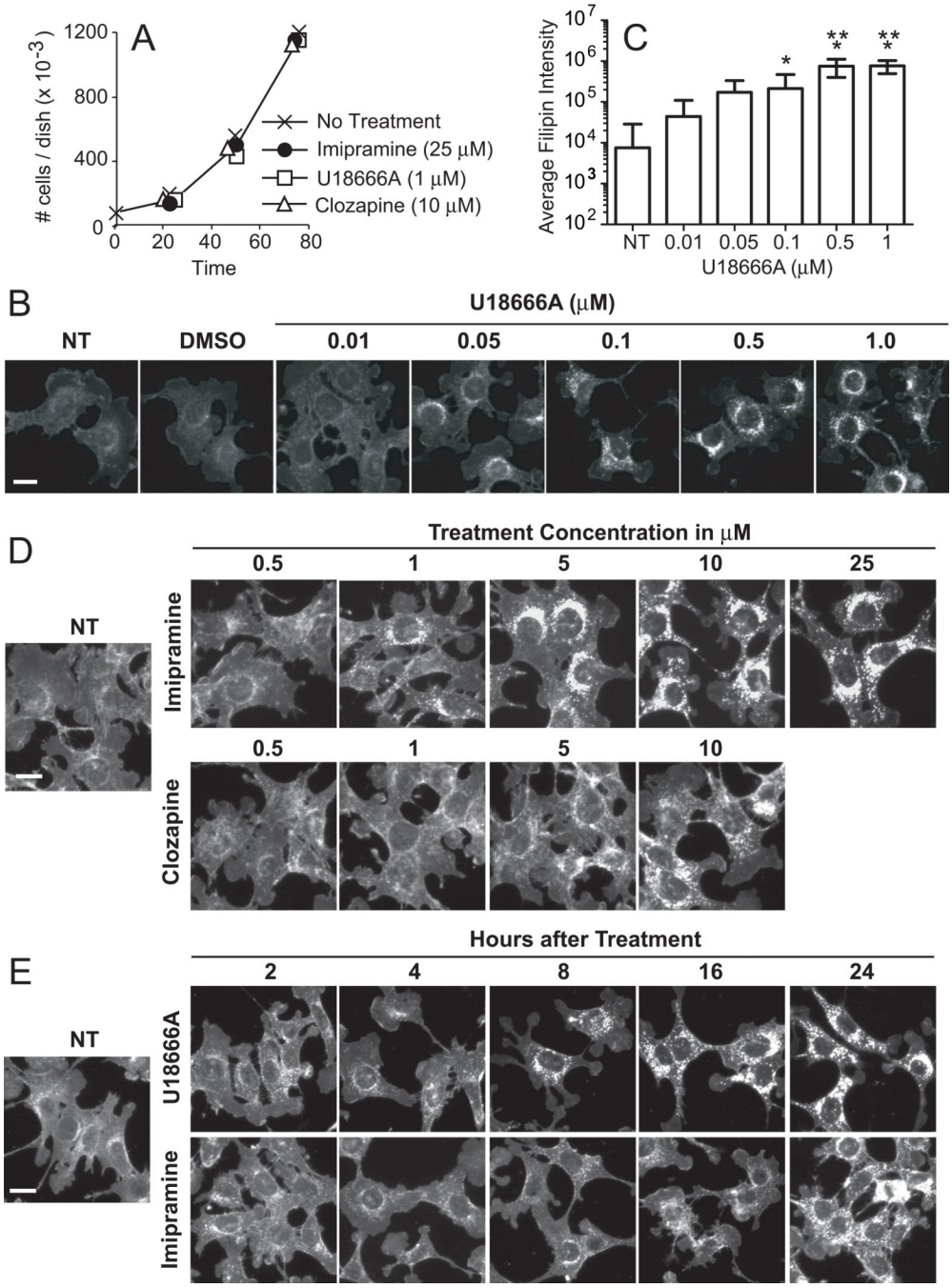


**Figure 1.**

Effects of U18666A, imipramine and clozapine on 1c1c7 cell growth and filipin staining. (A) Cultures of murine hepatoma 1c1c7 cells were treated with the indicated concentrations of U18666A, imipramine, or clozapine before being harvested and counted. Data represent means ± SD of three plates per treatment per time period. Similar results were obtained in a second independent experiment. (B) 1c1c7 cultures were treated with nothing (NT), DMSO or indicated concentrations of U18666A for ~24 h before being processed for filipin staining. (C) Quantification of per cell filipin fluorescence intensity in 1c1c7 cultures treated with U18666A for ~24 h. Data are from the experiment depicted in panel B and represent means ± SD of analyses of 18–35 cells for each treatment group. *Significantly greater than

non-treated (NT) control, $P<0.05$. **Significantly greater than 0.1 μM U18666A treatment group, $P<0.05$. (D) 1c1c7 cultures were treated with nothing or indicated concentrations of imipramine or clozapine for ~24 h before being stained with filipin. Similar patterns were observed in two additional experiments. (E) 1c1c7 cultures were treated with nothing or 1 μM U18666A or 25 μM imipramine for different lengths of time before being processed for filipin staining. White bar in panels B–E represents 20 microns.

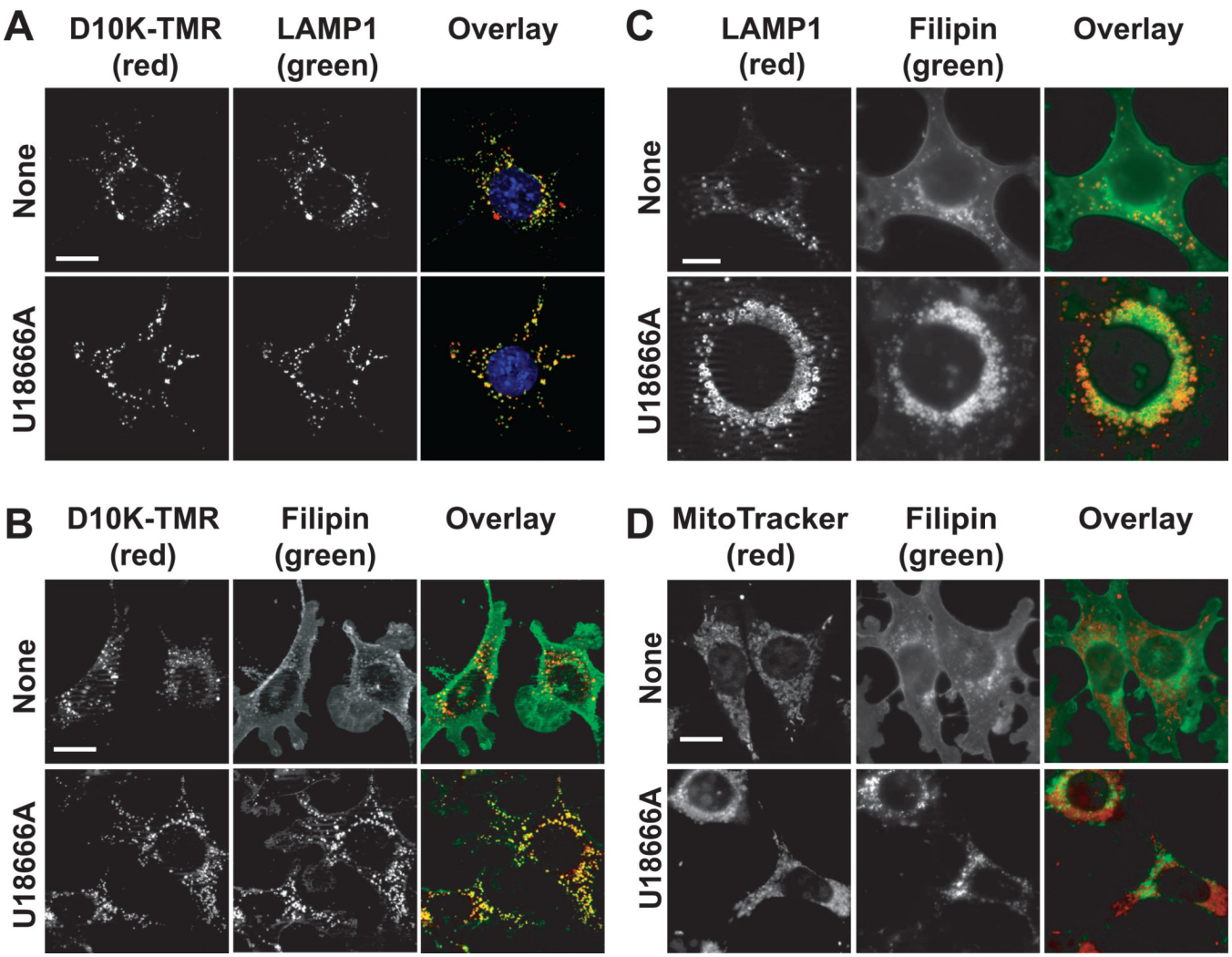


**Figure 2.**

U18666A-induced endosomal/ysosomal accumulation of non-esterified sterols. (A) 1c1c7 cultures were incubated with dextran-10000 tetramethylrhodamine (D10K-TMR) overnight prior to being washed and refed with fresh medium. At the time of refeeding some cultures were treated with 1 μM U18666A. After an additional 8 h of incubation the cultures were fixed and processed for detection of D10K-TMR (red) and LAMP1 (green). Colocalization of D10K-TMR and LAMP1 is indicated by orange – yellow punctate spots. (B) 1c1c7 cultures were incubated with D10K-TMR overnight prior to being washed, and refed with fresh medium. Some cultures were subsequently treated with 1 μM U18666A and incubated an additional 8 h before being stained with filipin. Colocalization of filipin (green) and D10K-TMR (red) structures is indicated by orange – yellow punctate spots. (C) 1c1c7 cultures were treated with nothing or 1 μM U18666A for 24 h prior to being fixed and processed for filipin (green) and LAMP1 (red) staining. (D) 1c1c7 cultures were treated with nothing or 1 μM U18666A for ~22 h prior to the addition of MitoTracker Green (MTG). After an additional 5 min of incubation cultures were washed, fixed and stained with filipin. The pictures presented in panels A–D are representative of what was observed in multiple fields of cells. White bar in panels A, B and D represents 20 microns. White bar in panel C represents 10 microns.

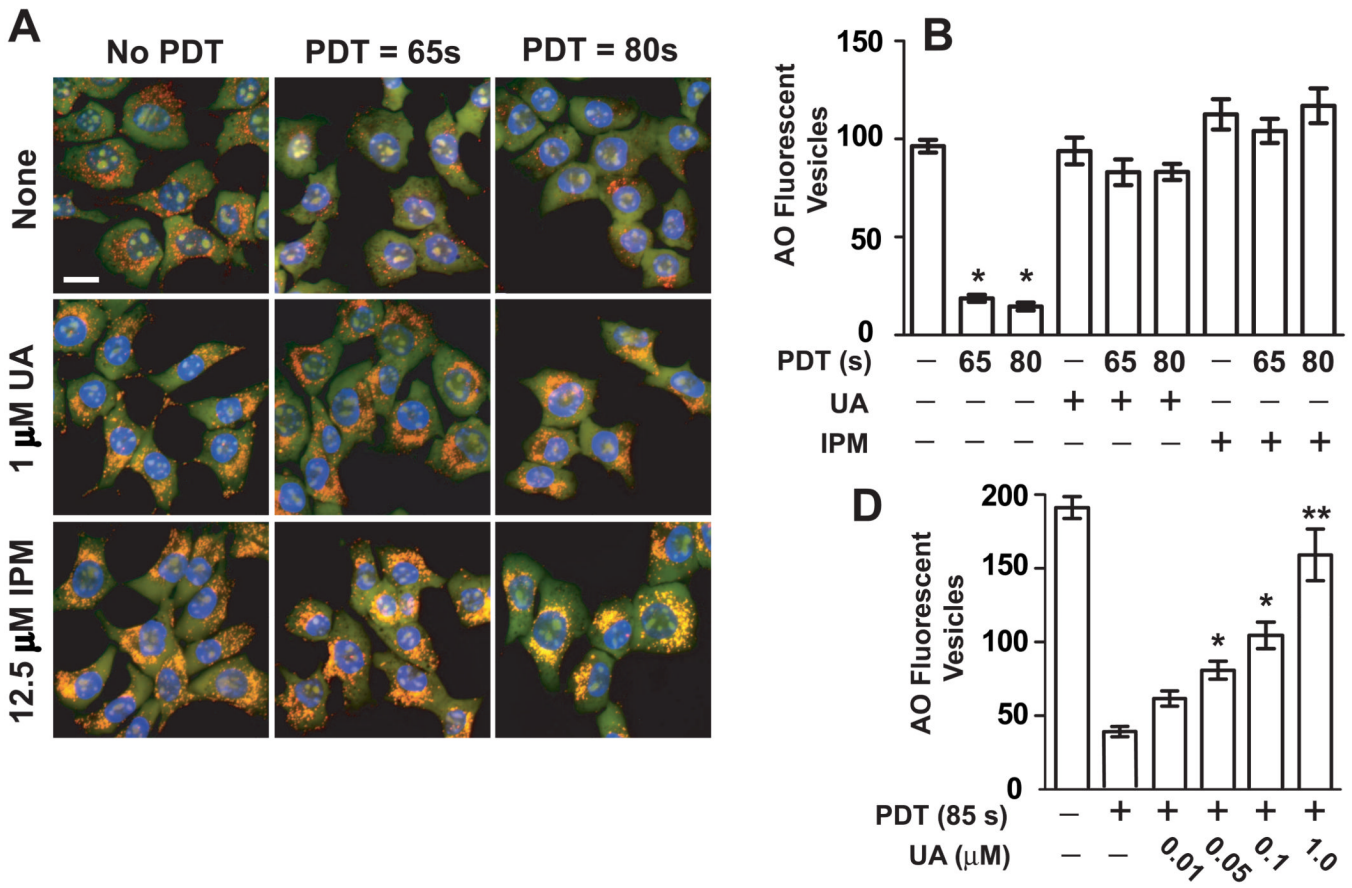


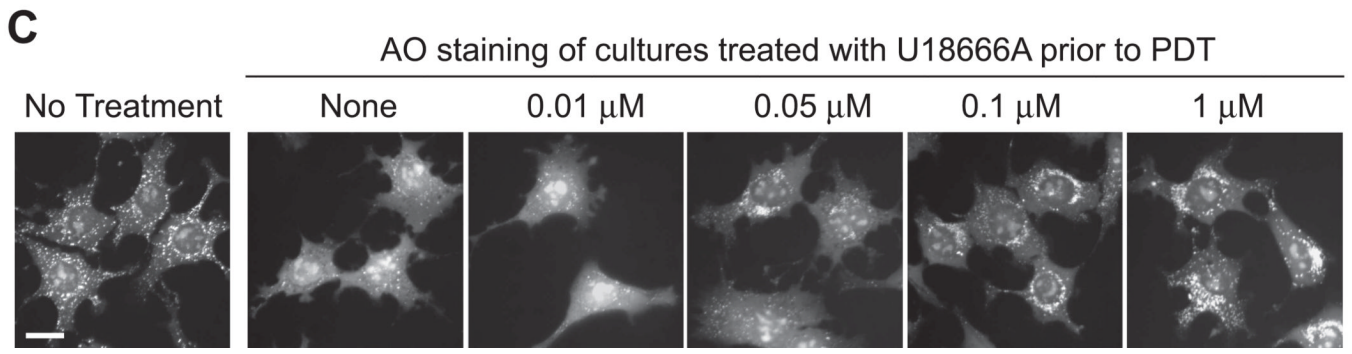


**Figure 3.**

CAD suppression of LMP. (A) 1c1c7 cultures were treated with nothing, 1 μM U18666A (UA), or 12.5 μM imipramine (IPM) for ~22 h prior to being washed and refed with fresh medium (± 33 μM NPe6 for 1 h) and subsequently photoirradiated for either 65 or 80 s. Sixty min after medium change the cultures were incubated with AO and HO33342 for ~10 min prior to being viewed by fluorescence microscopy. Treatment conditions are noted in the figure. The pictures presented in panel A are representative of what was observed in multiple fields of cells derived from 4 independent experiments. (B) Quantification of per cell AO-stained acidic vesicles observed in the experiment depicted in panel A. Data represent means ± SD of analyses of 10–12 cells per treatment group. *Significantly less than non-treated and all U18666A and imipramine treatment groups, $P<0.05$. (C) 1c1c7 cultures were pretreated for ~24 h with different concentrations of U18666A, or nothing, prior to being incubated with 33 μM NPe6 for 1 h, and then refed and photoirradiated.

Cultures were stained with AO ~1 h after photoirradiation, and imaged 10 min later. A parallel group received no treatment prior to AO staining. Similar results were observed in a second independent experiment. (D) Quantification of per cell AO-stained acidic vesicles observed in the experiment depicted in panel C. Data represent means ± SD of 15–20 cells per treatment group. *Significantly greater than PDT control, $P<0.05$. **Signficantly greater than all treatment groups except non-treated control, $P<0.05$. White bar in panels A and C represents 20 microns.

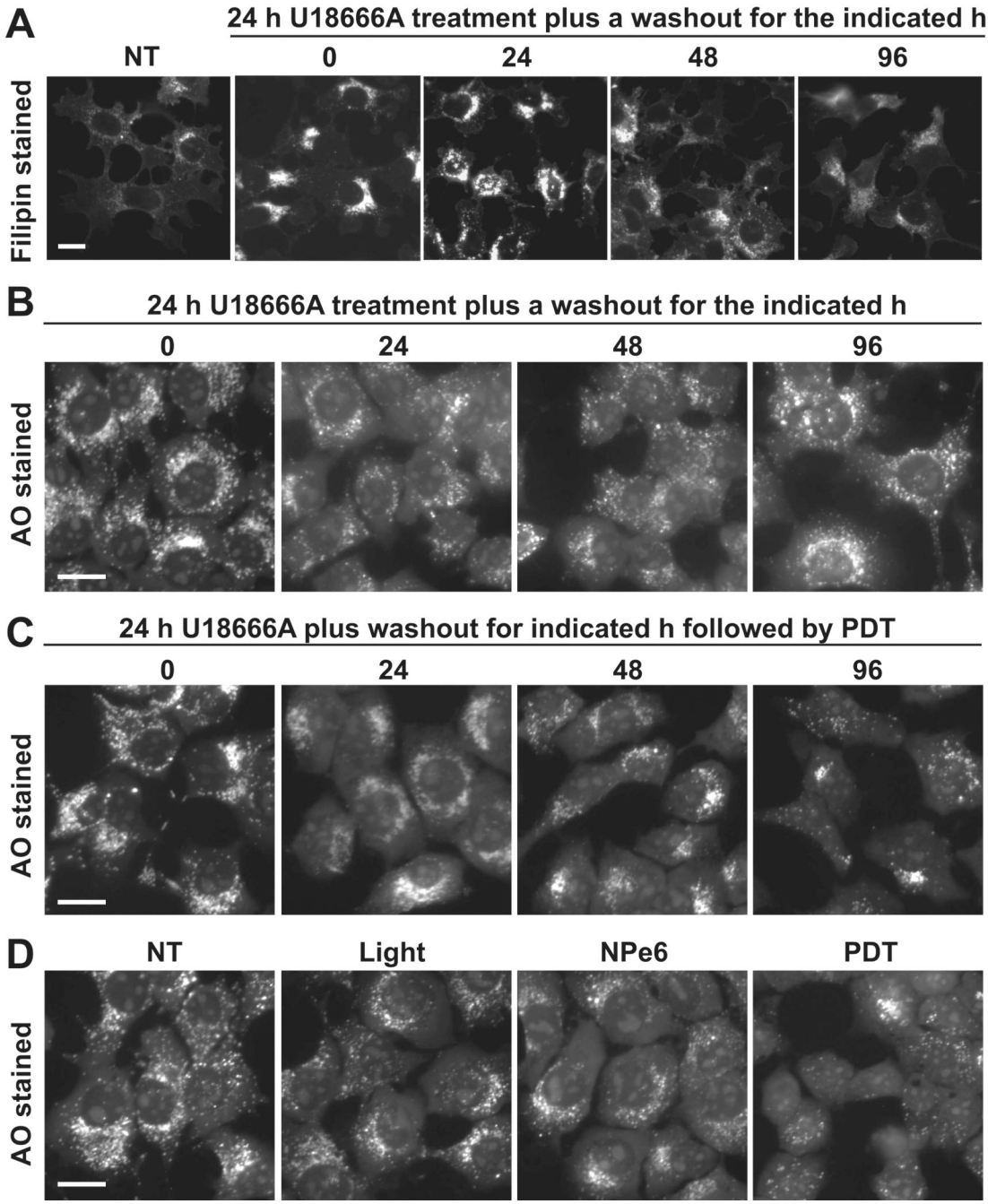


**Figure 4.**

Time-dependent recovery of sensitivity to PDT-induced LMP following washout of U18666A. (A) 1c1c7 cultures were treated with nothing (NT) or 1 μM U18666A for 24 h prior to being washed and refed with new medium lacking U18666A. Cultures were stained with filipin immediately prior to washout or 24, 48 and 96 h post medium change. (B) 1c1c7 cultures were treated with 1 μM U18666A for 24 h prior to being washed, and refed with new medium lacking U18666A. Some cultures were stained with AO either at the time of washout, or 24, 48 and 96 h post medium change. (C) A parallel set of cultures were sensitized with 33 μM NPe6 and photoirradiated prior to being stained with AO and monitored by fluorescence microscopy. Treatments are noted in the figure. (D) Some 1c1c7

cultures were treated with nothing, light only, or 33 μM NPe6 only for 1 h prior to being stained with AO. Additional cultures were loaded with NPe6 for 1 h, washed and refed, and irradiated. Cultures were stained with AO 1 h later. Treatments are noted in the figure. Results similar to those reported in panels A, B, C and D were obtained in 4, 2, 2 and 3 additional independent experiments, respectively. White bar represents 20 microns.

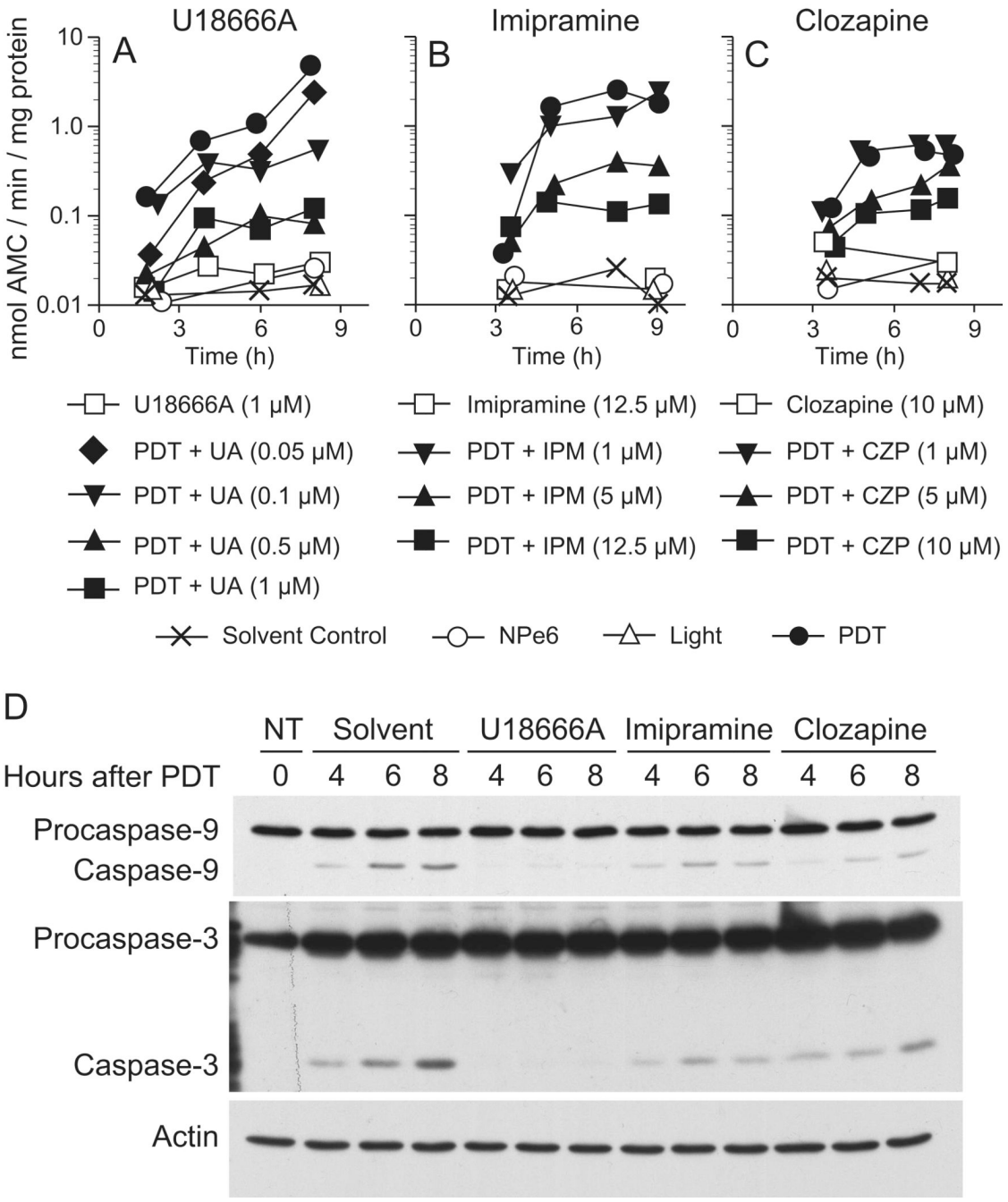


**Figure 5.**

U18666A-, imipramine- and clozapine-mediated inhibition of apoptosis initiated by photoirradiation of NPe6-sensitized cultures. 1c1c7 cultures were treated with nothing (NT) or different concentrations of U18666A (UA), imipramine (IPM), or clozapine (CZP) for ~24 h prior to being sensitized with 33 μM NPe6. Sensitized cultures were photoirradiated 1 h later for 80s. Cultures were harvested for analyses of DEVDase activities (A–C) or procaspase-9 and -3 cleavage (D) at indicated times after photoirradiation. Data in panels A–C represent means of triplicate analyses performed with the lysate of a single culture. The studies reported in panels A–C were repeated minimally a second time with similar results. The western blots in panel D employed 25 μg of cellular lysate per lane.

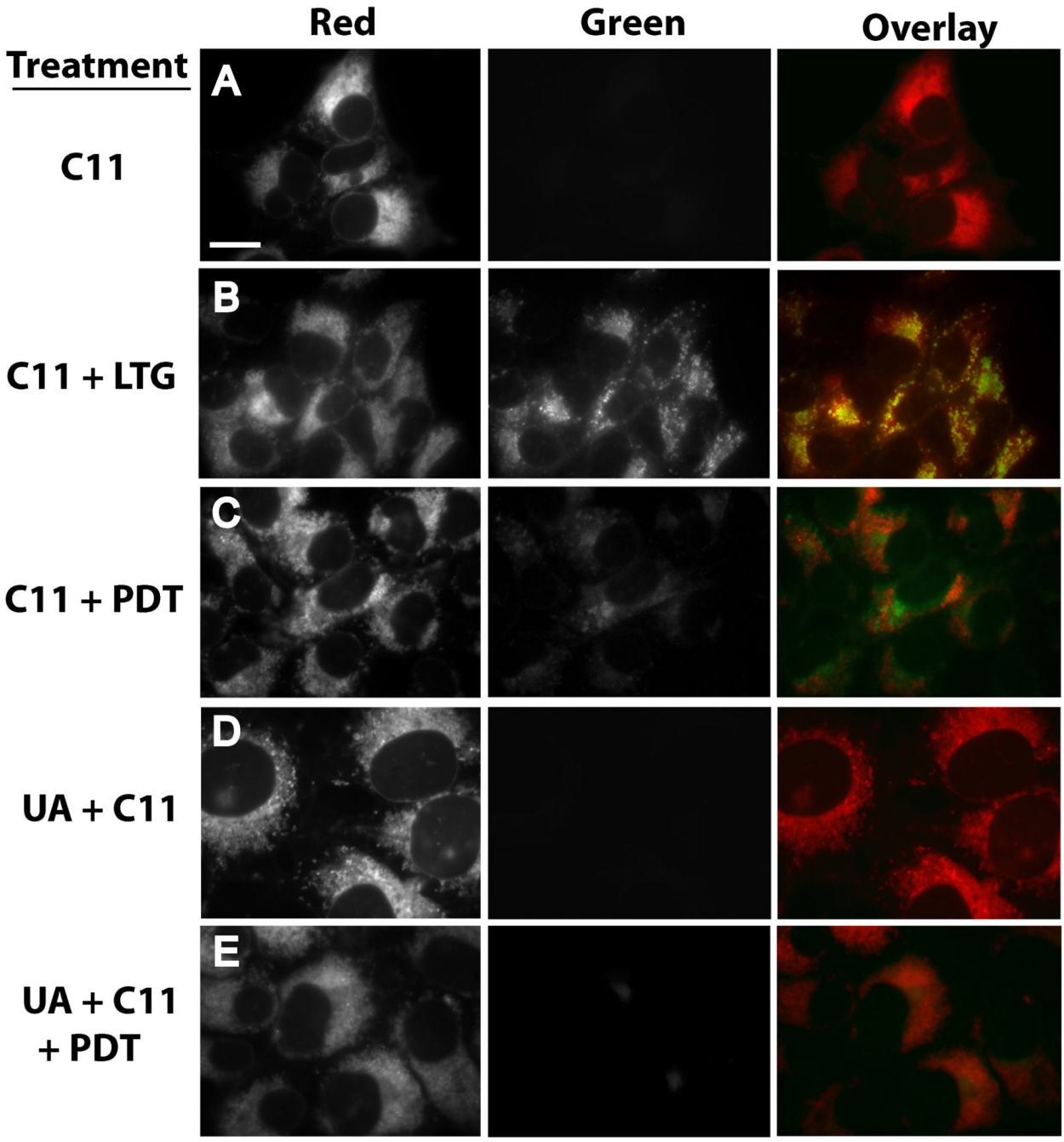


**Figure 6.**

U18666A suppresses PDT-induced oxidation of C11-BODIPY. (A) 1c1c7 cultures were exposed to 4 μM C11-BODIPY (C11) for 1 h prior to replacing medium and examination by fluorescence microscopy for the distribution of reduced (red) and oxidized (green) C11. (B) 1c1c7 cultures were treated with C11 as described above. LysoSensor Green (LSG, 2 μM) was added during the final 10 min of incubation. After changing the medium the cultures were imaged to capture red (C11) and green (LSG) fluorescence. C11 colocalization with LSG is indicated by the occurrence of punctate yellow/orange spots in the overlay. (C) Cultures were cotreated with 40 μM NPe6 and 4 μM C11 for 1 h prior to being washed, refed, and photoirradiated for 60s. After photoirradiation the cultures were immediately

imaged for detection of C11 fluorescence. (D) Cultures were treated with 0.75 μM U18666A for ~20 h prior to the addition of C11, and subsequently analyzed as described above. (E) Cultures were treated as in panel C except that they were incubated with 0.75 μM U18666A for ~20 h prior to the additions of NPe6 and C11. A second experiment yielded similar results for all treatment groups. White bar in panel A represents 20 microns.

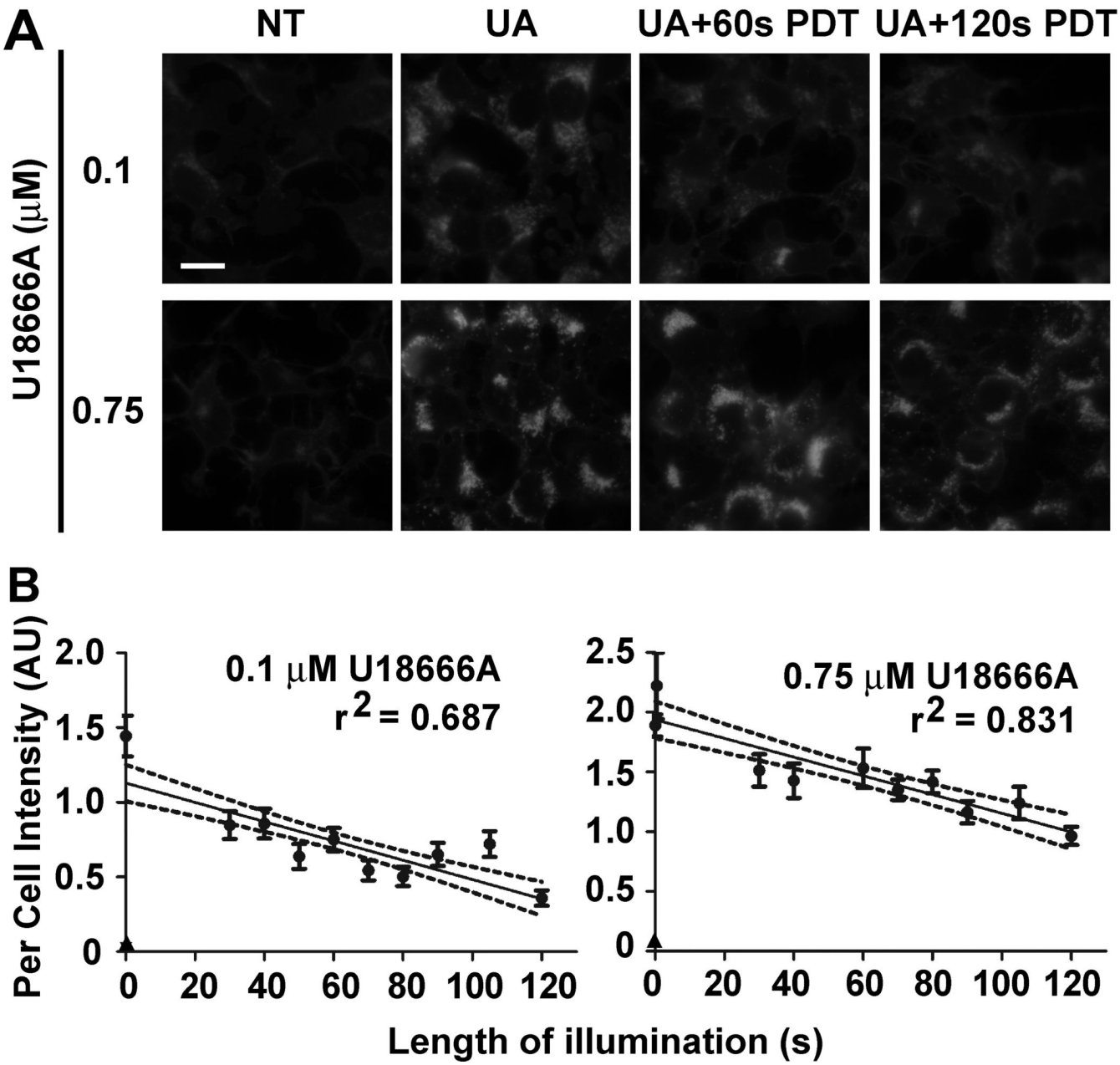


**Figure 7.**

PDT-induced oxidation of lysosomal cholesterol. (A) 1c1c7 cultures were not treated (NT) or exposed to 0.1 or 0.75 μM U18666A (UA) for ~20 h prior to being washed and refed with medium containing 33 μM NPe6. After 2 h of sensitization the cultures were washed, refed and photoirradiated for either 60 or 120 s. Cultures were fixed 30 min later and processed for filipin binding and fluorescence. White bar represents 20 microns. (B) Cultures were treated as described above except that photoirradiation times varied between 30 to 120 s. Data represent per cell filipin fluorescence intensities ± S.D. of 20–48 cells taken from multiple fields. The circles represent UA-treated cultures and the triangles represent NT cultures. The per cell filipin fluorescence intensity of every photoirradiated UA treatment group (at all light exposures) was statistically less ($P<0.05$) than the intensity measured in non-photoirradiated, UA-treated cultures. Results similar to that reported for cultures

pretreated with 0.75 μM UA were obtain in two additional experiments. Exposure settings for the capture of filipin fluorescence were uniform within an experiment, and initially set so as to yield a strong signal for non-irradiated, UA-treated cultures. The experiments involving pretreatment with either 0.1 or 0.75 μM UA18666A were performed and analyzed on different days. Hence, per cell intensity units are not directly comparable between experiments.

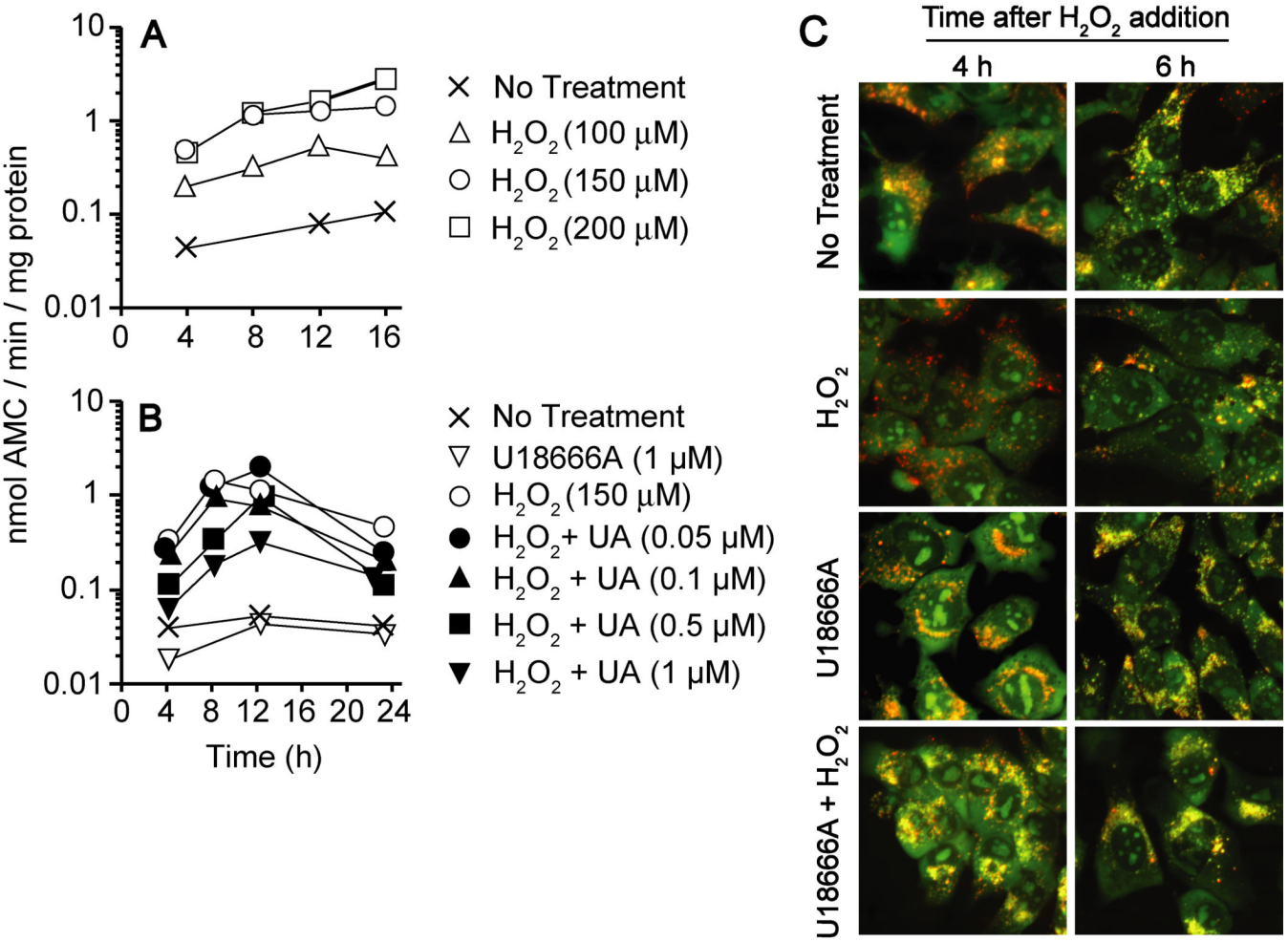


**Figure 8.**

U18666A-mediated suppression of $H_2O_2$-induced LMP and DEVDase activation. (A) 1c1c7 cultures were incubated with 100, 150 or 200 µM $H_2O_2$ for different lengths of time prior to being harvested for subsequent analyses of DEVDase activities. (B) 1c1c7 cultures were incubated with different concentrations of U18666A (UA) for ~24 h prior to being washed and refed with medium containing 150 µM $H_2O_2$. Cultures were harvested at various times after peroxide addition for analyses of DEVDase activities. Data in panels A and B represent means of triplicate analyses performed with the lysate of a single culture. Treatments are noted in the figure. Results similar to those reported in panels A and B were obtained in minimally three additional independent experiments. (C) 1c1c7 cultures were treated with nothing or 1 µM U18666A for ~20 h prior to being washed and refed with medium lacking or containing 150 µM $H_2O_2$. Cultures were stained with AO 4 or 6 h after medium change and monitored by fluorescence microscopy. Treatments are noted in the figure. Similar results were obtained in a second experiment. White bar represents 20 microns.

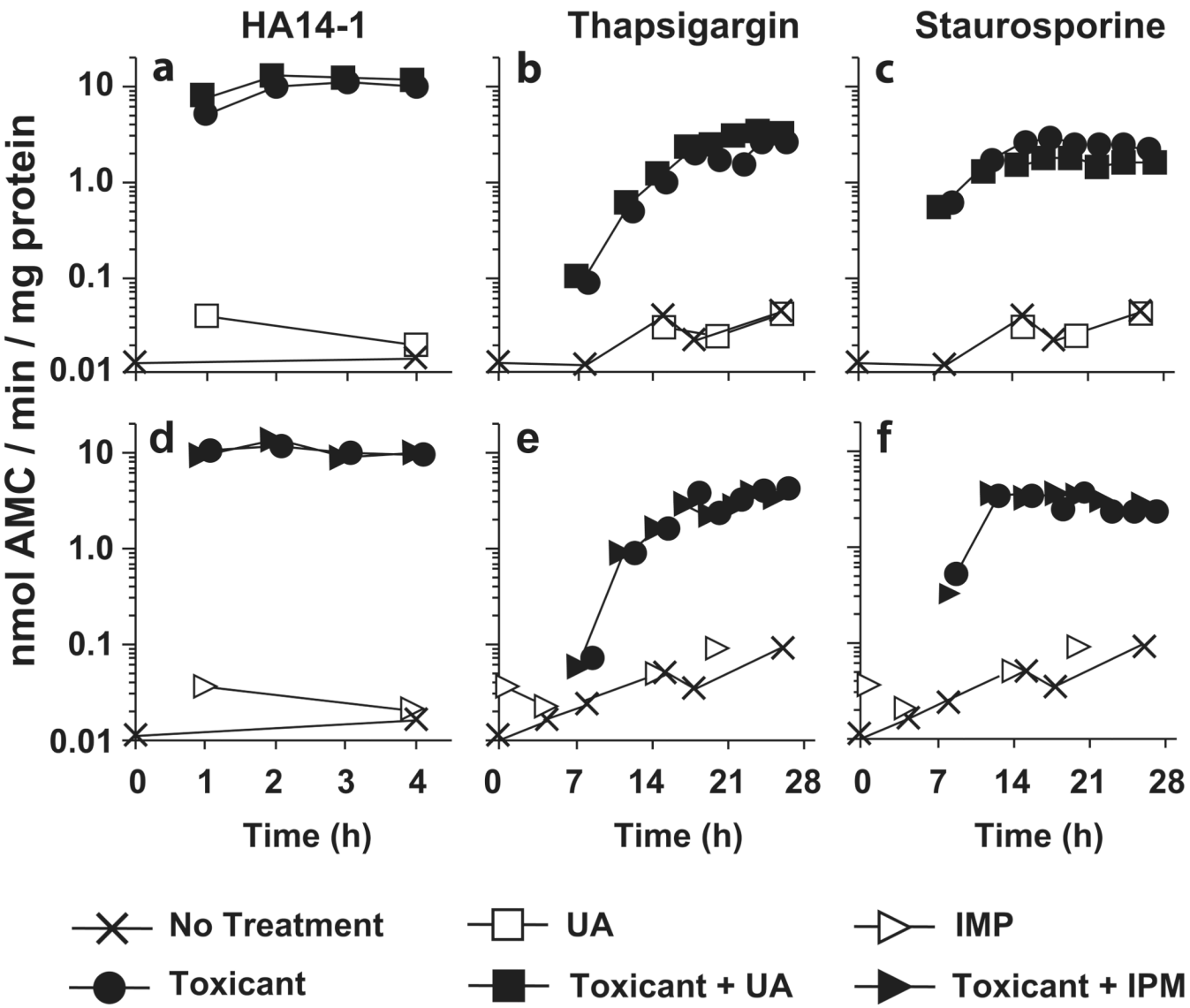


**Figure 9.**

U18666A does not suppress the pro-apoptotic activities of agents that do not induce LMP. 1c1c7 cultures were treated with nothing, 1 μM U18666A (UA), or 12.5 μM imipramine (IPM) for ~20 h. Some cultures were subsequently treated with 25 μM HA14-1 (A,D), 25 nM thapsigargin (B,E), or 100 nM staurosporine (C,F). Cultures were harvested at various times after toxicant treatment for analyses of DEVDase activities. Treatments are noted in the figure. Data points represent the means of triplicate analyses performed with the lysate of a single culture. Similar results were obtained in a second independent experiment.